2019

Fabrication and Characterization of Planar-Structure Perovskite Solar Cells

Guoduan Liu
University of Kentucky, guoduanliu@uky.edu
Digital Object Identifier: https://doi.org/10.13023/etd.2019.140

STUDENT AGREEMENT:

I represent that my thesis or dissertation and abstract are my original work. Proper attribution has been given to all outside sources. I understand that I am solely responsible for obtaining any needed copyright permissions. I have obtained needed written permission statement(s) from the owner(s) of each third-party copyrighted matter to be included in my work, allowing electronic distribution (if such use is not permitted by the fair use doctrine) which will be submitted to UKnowledge as Additional File.

I hereby grant to The University of Kentucky and its agents the irrevocable, non-exclusive, and royalty-free license to archive and make accessible my work in whole or in part in all forms of media, now or hereafter known. I agree that the document mentioned above may be made available immediately for worldwide access unless an embargo applies.

I retain all other ownership rights to the copyright of my work. I also retain the right to use in future works (such as articles or books) all or part of my work. I understand that I am free to register the copyright to my work.

REVIEW, APPROVAL AND ACCEPTANCE

The document mentioned above has been reviewed and accepted by the student's advisor, on behalf of the advisory committee, and by the Director of Graduate Studies (DGS), on behalf of the program; we verify that this is the final, approved version of the student's thesis including all changes required by the advisory committee. The undersigned agree to abide by the statements above.

Guoduan Liu, Student

Dr. Zhi David Chen, Major Professor

Dr. Aaron Cramer, Director of Graduate Studies

FABRICATION AND CHARACTERIZATION OF PLANAR-STRUCTURE PEROVSKITE SOLAR CELLS

THESIS

A thesis submitted in partial fulfillment of the
requirements for the degree of Master of Science in Electrical Engineering in the
College of Engineering
at the University of Kentucky

By

Guoduan Liu

Lexington, Kentucky

Director: Dr. Zhi David Chen, Professor of Electrical and Computer Engineering

Lexington, Kentucky

2019

https://orcid.org/0000-0001-2345-6789

ABSTRACT OF THESIS

FABRICATION AND CHARACTERIZATION OF PLANAR-STRUCTURE PEROVSKITE SOLAR CELLS

Currently organic-inorganic hybrid perovskite solar cells (PSCs) is one kind of promising photovoltaic technology due to low production cost, easy fabrication method and high power conversion efficiency.

Charge transport layers are found to be critical for device performance and stability. A traditional electron transport layer (ETL), such as TiO_2 (Titanium dioxide), is not very efficient for charge extraction at the interface. Compared with TiO_2, SnO_2 (Tin (IV) Oxide) possesses several advantages such as higher mobility and better energy level alignment. In addition, PSCs with planar structure can be processed at lower temperature compared to PSCs with other structures.

In this thesis, planar-structure perovskite solar cells with SnO_2 as the electron transport layer are fabricated. The one-step spin-coating method is employed for the fabrication. Several issues are studied such as annealing the samples in ambient air or glovebox, different concentration of solution used for the samples, the impact of using filter for solutions on samples. Finally, a reproducible fabrication procedure for planer-structure perovskite solar cells with an average power conversion efficiency of 16.8%, and a maximum power conversion efficiency of 18.1% is provided.

KEYWORDS: Planer-Structure Perovskite Solar Cells, Tin (IV) Oxide, Electron Transport Layer, Current-Voltage Measurement, Spin-Coating.

Guoduan Liu

(Name of Student)

04/16/2019

Date

FABRICATION AND CHARACTERIZATION OF PLANAR-STRUCTURE PEROVSKITE SOLAR CELLS

By
Guoduan Liu

Dr. Zhi David Chen
Director of Thesis

Dr. Aaron Cramer
Director of Graduate Studies

04/16/2019
Date

ACKNOWLEDGMENTS

Firstly, I would like to express my sincere gratitude to my advisor Dr. Zhi David Chen for the continuous support of my study and research. His critical and logical problem-solving strategies deeply influenced me.

Beside my advisor, I would like to thank the committee members for their time, insightful comments and questions.

Thank Dr. Vijay Singh for his great discussions, insightful comments, and for providing SnO2 target.

Thank Dr. Fuqian Yang for his help, discussion, and questions.

In addition, I would also like to thank Dr. Kenneth Graham at the Department of Chemistry for his discussion and for providing the UV-Ozone instrument and solar simulator and measurement system equipment.

Furthermore, I gratefully acknowledge all the members with whom I worked with in the lab including Dr. Hojjatollah Sarvari, Maniell Workman in our group.

Also, I would like to thank Somin Park and Ashkan Abtahi, Ph.D. students in Graham's lab since they offered help when we used their UV-Ozone instrument, J-V measurement system in our experiment

Last but not the least, I would like to thank my parents for supporting me in my life and study.

TABLE OF CONTENTS

LIST OF FIGURES

CHAPTER 1. PEROVSKITE SOLAR CELLS

1.1 Introduction

Today the world relies on fossil fuel resources such as coal, oil, and natural gases. Nevertheless, consuming fossil fuels can produce CO_2 and a great deal of pollutants, which cause global warming and environmental pollution. Thus, it is urgent to search for clean and renewable energy resources. Solar power is an attractive energy source since it is an entirely renewable source of energy that provides energy security, independence, and reliability.

Moreover, the sun is available all over the world freely as a source of energy, particularly in the southern states of the US. Solar power on Earth is the most abundant energy resource with a year's sunlight containing about 1.5×109 terawatt hour (TWh) of energy. In comparison, the total known reserves of oil, coal, and gas are only ~8.5×106 TWh. Thus, a year's solar power provides more than a hundred times the energy of the world's entire known fossil fuel resources (Sum and Mathews 2014). Harnessing solar energy could yield a stable energy supply. However, the difficulty is how to convert solar energy efficiently and cost-effectively. Sunlight is regarded as the most promising replacement for fossil fuels since it is a clean, cheap, abundant, and renewable energy source. One solar cell absorbs photons of incident light and converts the energy of light into electrical energy either by indirectly converting it to heat or directly based on the photovoltaic (PV) effect (Kearns and Calvin 1958). Most of the solar cells are designed to process sunlight that reaches the Earth's surface while others are optimized for use in the Space. Solar cells are working based on the PV effect that occurs when the light hits a semiconductor material and produces a potential difference or voltage. The voltage created in the cell produce a current through an external electrical circuit that is used to generate power. It is crucial to reduce the total cost of solar energy for making it competitive with the fossil fuels. Also, it can be achieved by either lowering the cost of PV cells or by increasing their power conversion efficiency (PCE). The performance of solar cells is evaluated by their PCE which calculated with the following formula 1-1 :

$$PCE = \frac{V_{OC} J_{SC} FF}{P_{IN}} \qquad FF = \frac{J_{m-pp} V_{m-pp}}{V_{OC} J_{SC}}$$

Where Voc is the open-circuit voltage, Jsc is the short-circuit current density, FF is the fill factor, Pin is the energy of incident light, Jm-pp is the current at the maximum power point and Vm-pp is the voltage at the maximum power point.

Organic-inorganic perovskites are currently the focus of semiconductor research with the promise to bring the next generation of highly efficient, cost-effective photovoltaic technology (Saliba, M. et.al. 2018). In only a few years, prototype devices designed on a lab scale demonstrated power conversion efficiency (PCE) of ≥20%. However, only a few research groups reported perovskite solar cells (PSCs) with PCEs higher than 20%, which used to be found in only the most established materials such as silicon, GaAs, CIGS, and CdTe (Saliba, M et.al. 2016, Shin, S. S et.al. 2017). While efficiencies are now approaching the thermodynamic limit, there is still incomplete knowledge of fundamental working and degradation mechanisms. A deeper understanding is critical to further improve device performances and long-term stability (Ibn-Mohammed et.al. 2017).

1.2 The Promise of Perovskite Solar Cells

Solar cells are mainly divided into three different generations. For the first generation of solar cells, it is made of crystalline silicon that contains materials such as polysilicon and monocrystalline silicon. They are the main solar cells in the solar market. Besides, silicon solar cells have the highest PCE up to now. The second generation solar cells are thin-film cells that contain amorphous silicon, cadmium telluride (CdTe), and CuInGaSe2 (CIGS) solar cells. Thin-film technology decreases the amount of active materials in a solar cell which leads to depressing the cost. Also, it is possible for thin-film solar cells to deposit cells on various substrates including flexible substrates for related applications. Recently, scientists have advanced the third-generation solar cells including organic solar cells, dye-sensitized solar cells (DSSCs), and perovskite solar cells (PSCs), in order to reduce the cost of the solar cells. There is much research invested into these emerging technologies such as DSSCs and PSCs, since they have the potential to achieve the goal of producing cost-effective and high-efficiency solar cells. The certified efficiency table for all generations PV cells (Chart) is shown by Figure 1-1. The best certified PCE belongs to four junction silicon solar cell with η =44.7%. CIGS technology reaches the efficiency as high as 21%. Currently, Cu_2ZnSnS_4 (CZTS) solar cells emerged with the less-toxic thin film solar cell technology, which achieved about

12% efficiency. Among the third-generation solar cells, the PCE of PSCs has increased from 3.81% to over 24.2% from 2009 to 2018 (Kojima, Teshima et al. 2009, NREL Best Research-Cells Efficiencies,2019).

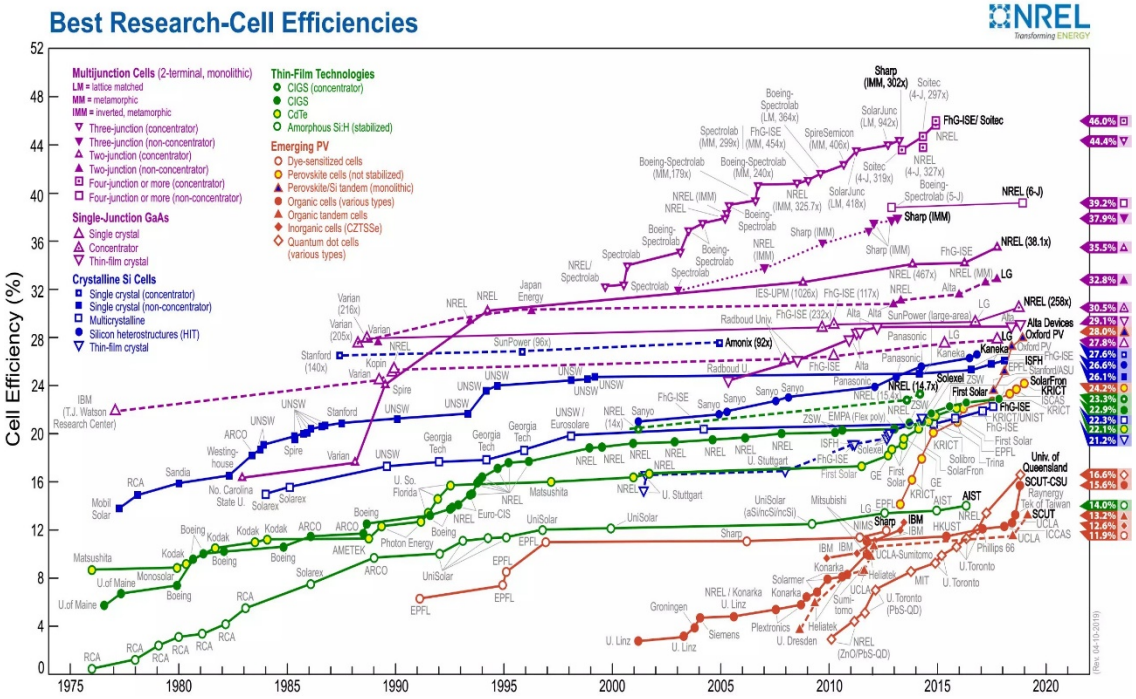

Figure 1.1 Best research-cell efficiencies. (NREL Best Research-Cells Efficiencies, 2019).

Furthermore, solar cells can be categorized into three types according to the materials that were used for absorption layers: inorganic, organic, and hybrid. For example, inorganic solar cells, such as silicon-based and III-V compound based, are main solar cells in the market. Nevertheless, the manufacturing processes are usually expensive. Organic solar cells contain polymer-based and small molecule-based types. The scientist Tang et al. invented the first organic solar cell in 1986. Currently organic solar cells did not entered the commercial market, since their efficiency is extremely low compared to others (Green, Emery et al. 2011). Hybrid solar cells use inorganic-organic halide perovskite as the absorber layer in their structure, and the light absorber of the PSCs is $APbX_3$ ($A=CH_3NH_3$, $(NH_2)_2CH_2$ or Cs, X= I, Br or Cl) film. PSCs are considered as the most

promising replacement of silicon solar cells because of their cost-effective and high absorption properties. Perovskite was firstly discovered in the Ural Mountains of Russia by Gustav Rose in 1839, and then is named after the Russian mineralogist Lev Perovski (1792–1856). Its name derived from a class of compounds that have the same type of crystal structure as $CaTiO_3$ (ABO_3, ABX_3), which is known as the perovskite structure (Wenk and Bulakh 2016).

Perovskite structure has many excellent properties, such as the option of low-temperature processing, tunable band gap, low production cost, high absorption coefficient, etc. For example, halide perovskites own the ideal band gap range from 1.2 eV to 2.3 eV which can be adjusted by the materials composition. Besides, perovskites possess high absorption coefficient, which indicates that only several hundreds of nanometers of perovskite are enough to collect sufficient light. Also, this material has long electron and hole diffusion lengths, which are essential for high-performance solar cells to suppress the recombination of photo excited charges.

As light harvesters and hole transport materials, organic-inorganic lead (Pb) halide perovskites have revolutionized the emerging PV technologies since the solar cells can be manufactured using cost-effective solution-based processes (Lee, Teuscher et al. 2012, Burschka, Pellet et al. 2013, Liu, Johnston et al. 2013, Im, Jang et al. 2014, Zhou, Chen et al. 2014, Yang, Park et al. 2017). Kojima Group firstly reported combination of perovskites into a solar cell in 2009 (Kojima, Teshima et al. 2009). This cell was based on a dye-sensitized solar cell, which produced 3.81% PCE with a thin layer of $CH_3NH_3PbI_3$ and 3.13% PCE with a thin layer of $CH_3NH_3PbI_3$ on mesoporous TiO_2 as electron-collector. In 2011, Park et al. improved the structure of the PSCs and achieved a

PCE of 6.5% (Im, Lee et al. 2011). In 2013, J. Burschka et al. used the sequential deposition method as a new pathway for the fabrication of PSCs to optimize the morphology of perovskite layer, and the certified PCE of 14.14% for the champion cell with the average of 12% in reverse scan measurement was reached (Burschka, Pellet et al. 2013). After then, excellent research about high efficiencies in organic-inorganic lead halide PSCs have been reported with maximum efficiencies over 22% (Bi, Tress et al. 2016, Liu, Li et al. 2017, Yang, Park et al. 2017), exhibiting promising potential of perovskite materials toward future cost-effective and high-performance solar cells.

1.3 Crystal Structure of Perovskite

Perovskite crystal structure is firstly described by Victor Goldschmidt in his research on tolerance factors in 1926 (Goldschmidt 1926). Perovskites own a cubic structure with a general formula of ABO_3 or ABX_3, and ABO_3 are oxide perovskites. They are colorless and wide band gap solids. Therefore, oxide perovskites are unwanted for high-efficiency solar cells. ABX_3 are halide perovskites that can merely accomplish band gap tuning by varying of all three cation and anion components. In ABX_3 perovskites, the eight A-site ions located on the eight corners of the lattice, a B-site ion, in the center of the lattice, and six X-atoms on the six faces. Figure 1.2 illustrates the unit cell of most commonly studied inorganic-organic halide perovskite Methylammonium lead tri-halide ($CH_3NH_3PbX_3$). A is a small monovalent organic cation such as methylammonium (CH_3NH_3) on the corners of the lattice. B is a divalent group 14 metal (Ge, Sn or Pb) in the center of the lattice and X are halides (Cl, Br or I). $CH_3NH_3PbX_3$ owns a band gap between 1.55 eV and 2.3 eV. The band gap is manageable by changing the halide content (Eperon, Stranks et al. 2014).

This type of perovskite can harvest the energy of sunlight efficiently as it absorbs both visible and infrared light.

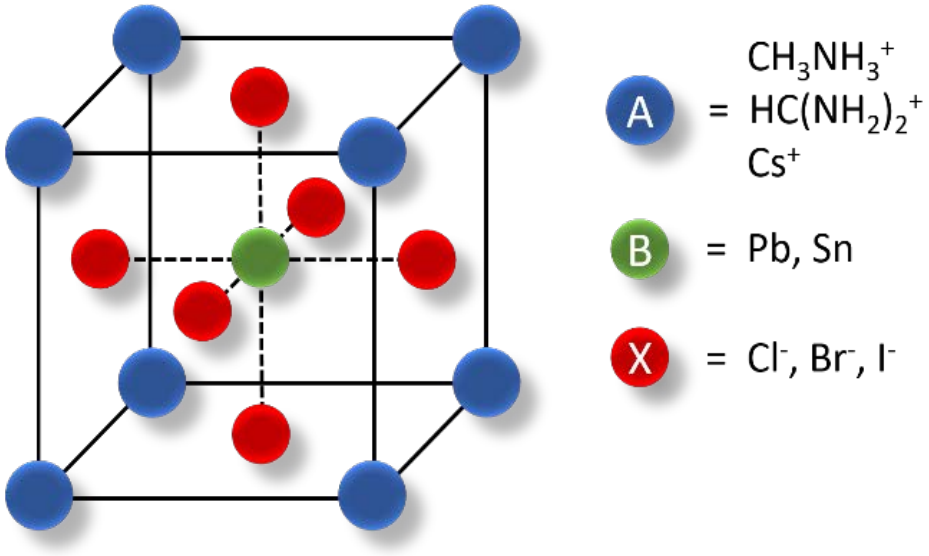

Figure 1.2 Unit cell of inorganic-organic halide perovskite CH3NH3PbX3, where X is I, Br or Cl ((Eperon, Stranks et al. 2014).

1.4 Device Structure and the Operational Principle of Planar PSCs

According to containing mesoporous layer or not, there are planar and mesoporous structures for PSCs. The planar PSCs are categorized in two forms such as planar regular and planar inverted PSCs, which is shown in the Figure 1.3. The planar structure consists of transparent conductive electrode such as Fluorine-doped thin oxide (FTO) or indium tin oxide (ITO)/ electron transport layer (ETL) as n-region/ perovskite absorber layer (intrinsic)/ hole-transporting layer as p-region, which is the structure of n-i-p. In this thesis, we focused on the regular planar PSC that does not include a mesoporous layer on top of the n-type region. This structure contains a substrate made of FTO on the top of a piece of glass. Light must go through this layer to reach the center of the device, so the glass and FTO must be low resistance and high-transmittance without reducing the light

power. On top of FTO, we have a thin layer as the electron transport layer (ETL), this layer is the n-type region of the n-i-p structure. Also, the absorbing perovskite layer work as the intrinsic region. Besides, the hole transport material (HTM) is spiro-OMeTAD that is an organic material doped with other additives, which serve as the p-type region on top of perovskite in the n-i-p structure. Finally, a thin layer of gold (Au) is used as the metal contact in order to collect the holes and connect with the electrodes. The principle of operation is as follows: the incidence of photons into perovskite generates electron-hole pairs. Electrons arrived at the electron transport layer. Next, electrons are collected by the FTO substrate. Meanwhile, the holes that are injected into the HTL (hole transport layer), eventually collected by the Au electrode.

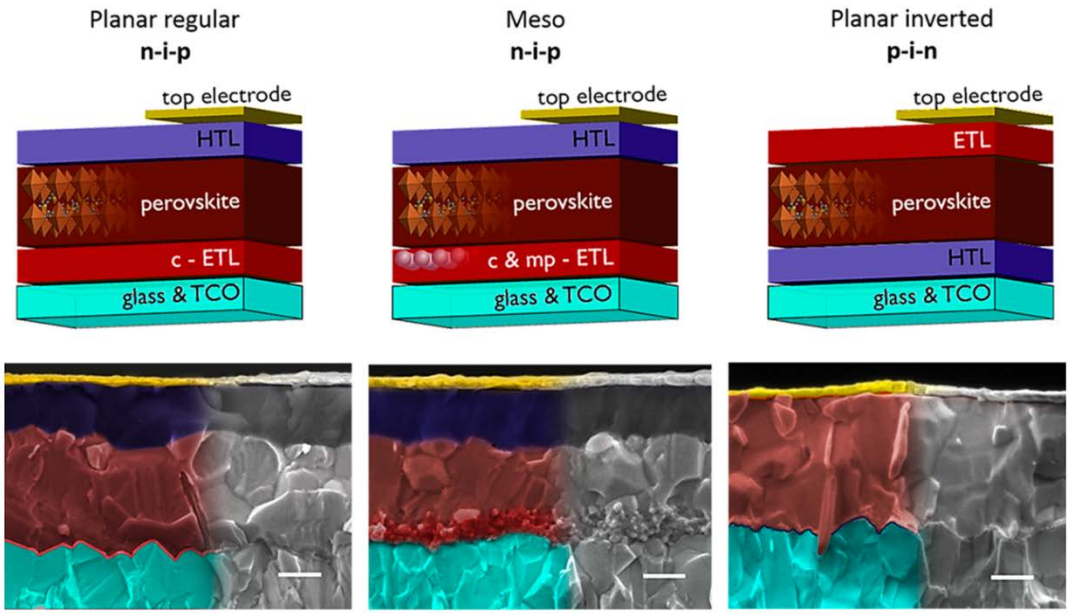

Figure 1.3 Schematics of the three PSC architectures, and corresponding SEM crossing-section images of representative devices are shown below with a scale bar of 200 nm (Michael Saliba et al. 2018).

CHAPTER 2. FABRICATION METHODS OF PEROVSKITE SOLAR CELLS

In this chapter, fabrication and deposition methods are discussed in this thesis. For instance, here we used RF sputtering, spin-coating methods for the deposition of a thin SnO_2 as the ETL. These methods are explained in detail under deposition of ETL section.

The chemicals we used were purchased from Sigma-Aldrich. All solvents were anhydrous. The Spiro-OMeTAD was purchased from Borun New Materials, LLC. The MAI, TiO_2 paste (18-NRZ), FAI, FK209, MABr, and FABr materials were purchased from Great cell Solar Ltd. FTO coated glass (Pilkington, $15\Omega.cm^{-2}$) was used as the substrate.

2.1 Fluorine-doped Tin Oxide (FTO)

Fluorine-doped Tin Oxide (FTO) is used as the substrate in our solar cells, since compared to the ITO, it has excellent stability at high temperatures, low cost, and keeps high transmittance (> 80%) at low resistance. The work function of FTO was about 4.4 eV (Andersson, Johansson et al. 1998). However, recent studies matching with new cleaning processes found a higher work function of 5 eV for FTO substrates (Helander, Greiner et al. 2011). ITO with a band gap of 3.5-4.3 eV that owns excellent electrical conductivity and optical transparency is another widely used substrate for PSCs. ITO can also be deposited as a thin film and provides a smoother surface compared to the FTO substrate. Here we used FTO as a substrate in this thesis.

2.1.1 Sonication in Solvents

Cleaning of the substrate is an important step in the fabrication of PSCs, since it will affect the performance of the device significantly. Several cleaning process steps must be done in order to clean the FTO substrate correctly. For instance, cleaning FTO substrates with only acetone and IPA will cause high carbon contamination on the surface of FTO (Helander, Greiner et al. 2011). These contaminations will decrease the work function of FTO, which causes non-ideal band alignment in the band structure of PSCs. Therefore, we need to optimize the procedure during the cleaning of samples. A typical cleaning process includes washing substrates with hand soap detergent, and then sonication in a solution of Hellmanex III and DI water (2:10 volume ratio) for 30 min, after that, sonication with acetone, IPA, and DI water for 15 min each at a temperature of 50℃. Also, the substrates must be washed with DI water thoroughly after sonication in Hellmanex III solution. This step is very important, otherwise, the samples will show cloudy non-uniform regions on the surface, and these non-idealities will decrease the light transmission through the glass and FTO layer. Besides, we usually use the boiling DI water to rinse and clean the substrates. After sonication with IPA, samples dried with the N_2 flow and kept in the room temperature for immediate use in the next step of experiments. We used the profiler (Figure 2.1) to check the surface of the substrates, and the clean surface of the substrates are shown in the graphs below:

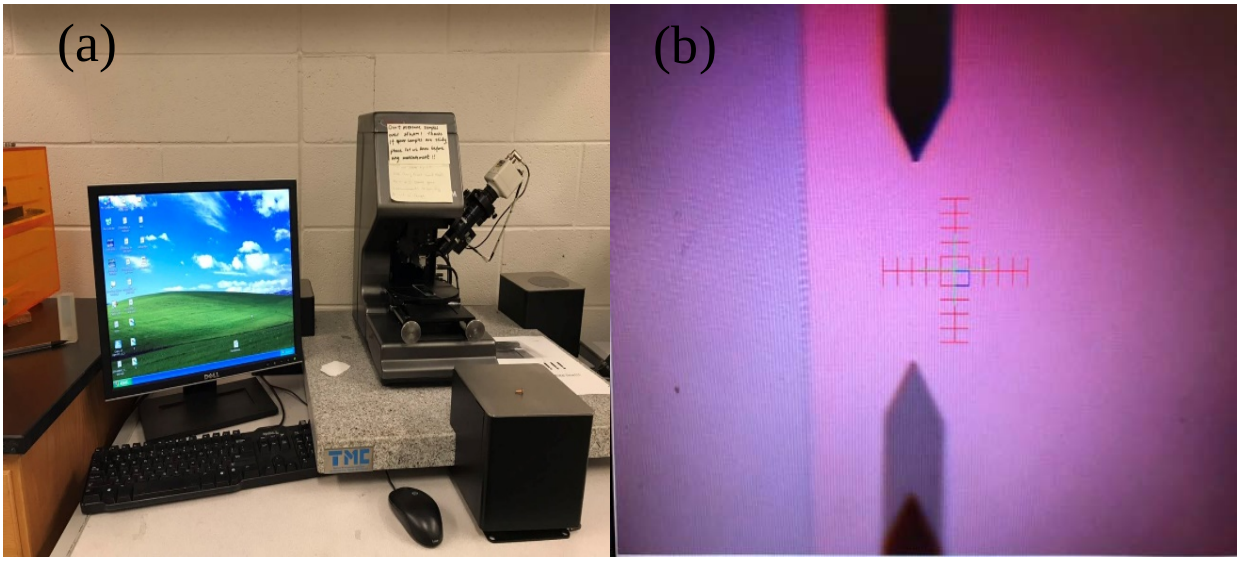

Figure 2.1 Profiler for checking the cleanness of FTO substrate and the clean surface of substrates under profiler.

2.1.2 UV Ozone Treatment

It is crucial to own a smooth, spike-free FTO surface especially when the next top layer is a (~30-60 nm) thin film. UVO treatment is applied to the FTO samples before Electron transport Layer spinning coating and Perovskite layer spinning coating, because this etching process provides smoother surface compared to the non-etched samples. In addition, UV-Ozone treatment is necessary for removing the residuals in the electron transport layer such as SnO_2 films and enhancing the wettability before perovskite depositing. Thus, in this thesis, we usually use the UVO treatment for 15 min for samples right before spinning coating of the SnO_2 electron transport layer and perovskite layer. Also, the UVO treatment is provided by Graham lab at the Department of Chemistry at the University of Kentucky. The graph below shows the UVO instrument:

Figure 2.2 The UV-Ozone Cleaner.

2.2 Electron Transport Layer

The existence of electron transport layer (ETL) is vital for the performance of PSCs. It prevents generated holes from reaching the substrate and transport electrons toward the substrate. The ideal film is a thin layer of materials that can cover the entire surface of substrate without any micro/nano pinholes. The full coverage of surface depends on the factor such as deposition technique. Also, a traditional electron transport layer (ETL), such as TiO_2, is not very efficient for charge extraction at the interface, especially in planar structure. In addition, the devices using TiO_2 suffer from serious degradation under ultraviolet illumination.

Compared with TiO_2, SnO_2 possesses several advantages such as higher mobility and better energy level alignment. More importantly, use of SnO_2 as ETL can eliminate/minimize degradation of perovskite solar cells induced by TiO_2 ETL, leading to significantly enhanced operational lifetime under continuous light illumination. Besides,

in contrast with TiO_2, SnO_2 could be easily coated by low temperature solution process, electrodeposition process, atomic layer deposition, chemical bath deposition, electron-beam deposition, and sputtering deposition.

SnO_2 has attracted great attentions as ETL for PSCs, and it is considered as the most promising alternative to TiO_2 due to following reasons: 1) SnO_2 possesses deep conduction band and good energy level as shown in Figure 2.3 (A.J. Nozik, R.Memming, J.Phys. Chem.1996,100 13061). The excellent band energy at ETL and perovskite interface will enhance electron extraction and hole blocking. 2) SnO_2 preserves high bulk electron mobility of up to 240 cm2 V-1s-1 and high conductivity, which can greatly improve the electron transport efficiency and reduce the recommendation loss. 3) SnO_2 has wide optical bandgap (3.6-4.0 eV) and high transmittance over the whole visible spectra, which can keep most of light pass through and be absorbed by the perovskite layer. 4) SnO_2 is easily processed by low-temperature methods (<200℃), which is compatible with flexible solar cells, tandem solar cells and large-scale commercialization. 5) SnO_2 showed outstanding chemical stability, UV-resistance properties, and less photocatalytic activity in comparison with TiO_2 or other ETLs, which is supportive for overall device stability.

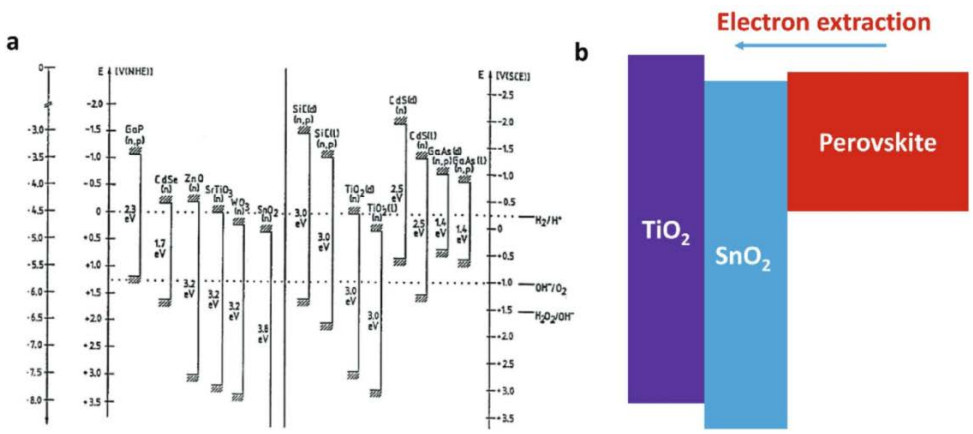

Figure 2.3 a) Energy level diagram of various electron transport layer. b) Band alignment of SnO_2, TiO_2 and perovskite layer. (Qi Jiang et al. 2018).

2.3 Brief history of SnO_2 as ETL for PSCs

SnO_2 has been tried to be used in organic solar cells and dye sensitized solar cells in previous research; however, the device performance is not as good as using ZnO and TiO_2 in these two kinds of devices. In 2015, several groups independently employed SnO_2 in PSCs. For instance, Dai team used mesoporous SnO_2 nanoparticle films as ETL by combining with $TiCl_4$ treatment, they got efficiency of 10.18%. Ma group used SnO_2 as condense layer and combined with TiO_2 mesoporous layer as ETL and achieved PCE of 7.43%. Later on, Kuang team used $TiCl_4$ treated SnO_2 nanocolloidal film as ETL and a PCE of 14.69% was obtained. Although these significant progresses in SnO_2 based perovskite solar cells have been obtained, the performance are still much lower than the devices usingTiO_2 as ETL. This might be attributed to the existence of large amount of charge traps or recombination centers such as oxygen vacancies in SnO_2 layer, which were caused by high temperature annealing (450℃).

To avoid the defects induced by high temperature processing, low temperature processed SnO_2 has been developed. Tian team employed SnO_2 thin film by spin-coating SnO2 nanoparticles on substrates followed by annealing at 200℃, a 13% PCE was achieved. Fang reported a big step for SnO_2-based PSCs, they adopted thermal decomposition of $SnCl_2{\cdot}2H_2O$ precursor at 180℃ in ambient air to form SnO_2 film on FTO substrate and achieved 17.21% reverse scan efficiency. Later on, Hagfeldt group used a low

temperature atomic layer deposition (ALD) process to grow SnO_2 ETL and showed the PCE above 18% with Voc exceeding 1.19 V. The devices performance is still lag behind TiO_2 devices at that time. Later You group employed high quality SnO_2 nanocrystal colloidal as ETL and annealed under moderate temperature (150℃), a certified efficiency of 19.9% with almost free of hysteresis of planar structure perovskite solar cells have been achieved. Meanwhile, Hagfeldt team reported a 20.7% PCE measured in house using double layer SnO_2 fabricated by spin coating and CBD method. More recently, You group reported the efficiency of SnO_2-based PSCs has been achieved 21.6% through finely controlling the surface passivation layer of PbI2 and the certificated efficiency of 20.9% has reached. The main achievements in perovskite solar cells for different groups using SnO_2 as electron transport layer are shown in Figure 2.4(Qi Jiang et. al. Small, 2018).

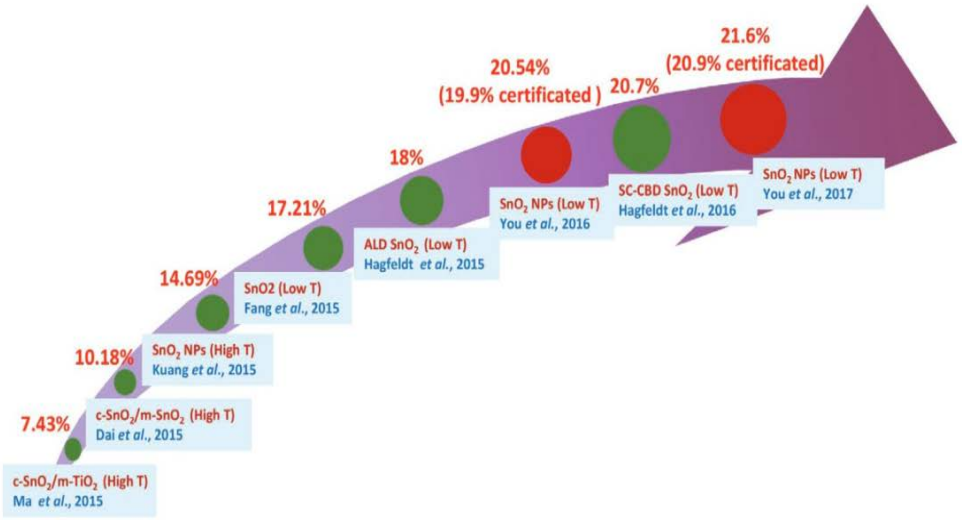

Figure 2.4 The main achievements in perovskite solar cells using SnO_2 as electron transport layer for different groups. (Qi Jiang et al. 2018).

2.4 Growth Method of SnO_2

Several advanced technologies can be used to deposit SnO_2 layer such as solution process method, sputtering deposition method, atomic layer deposition method, chemical bath deposition method and other methods.

In this thesis, we tried different methods for deposition of SnO_2 as the ETL layer such as RF sputtering method, solution process method. The details of each method are provided in the relevant subsection.

2.4.1 Sputtering Deposition Method for ELT Layer

Sputtering deposition method was used to deposit a thin, compact layer of SnO_2 with SnO_2 target. The crystallization of SnO_2 can be formed during the depositing period on the substrates, and usually post thermal annealing was not needed, which is good for flexible device fabrication. Currently about 19.8% PCE have been obtained by using spurting deposition, but this method may cost more such as oxygen and time for fabrication. Here, this method was tried, but the PCE is not good due to oxygen resource. This issue is described in the following section. The sputtering system is shown in the graph below:

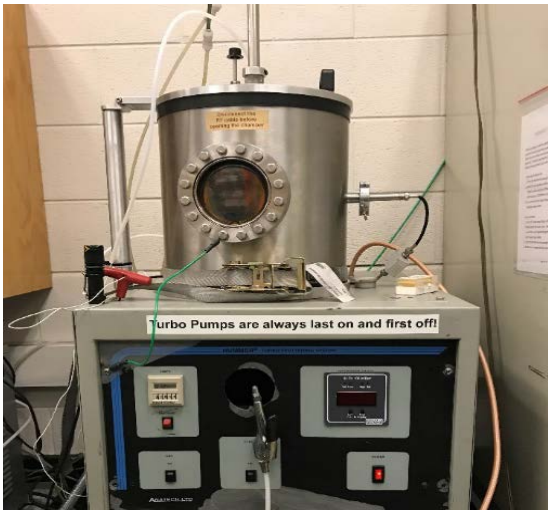

Figure 2.5 Sputtering deposition system.

2.4.2 Solution Process Method for ETL layer

Solution process is the common method for depositing SnO_2 layer by either thermal decomposition of Sn-based salt precursor or synthesizing SnO_2 nanocolloidals. For thermal decompositions, $SnCl_2$, $SnCl_4$, or their hydrate $SnCl_2 \cdot 2H_2O$, $SnCl_4 \cdot 5H_2O$ was dissolved in ethanol or other solvents, and then the precursor solution was spin coated on substrate and thermal annealing is needed in ambient air to convert into SnO_2. (Qi Jiang et. al. Small, 2018, Qi Jiang et. al. Advanced Materials, 2017).

In this thesis, we mainly used solution process method to form SnO_2 layer; also using the spin-coater placed inside the glovebox. The results for PSCs based on different solutions along with the optimization of the process are provided in Chapter 3. The SnO_2 colloid precursor was obtained from Alfa Aesar (tin (IV) oxide. For this SnO_2, one is said 15% in H_2O colloidal dispersion, the other said the accurate concentration is 20%. So we compared the performance of perovskite solar cells using two kinds of SnO_2 solution in the further experiments. For solution 1, we mixed 267μL of SnO_2 mixed with 1730 μL of water. For solution 2, we mixed 333μL of SnO_2 mixed with 1670 μL of water. Usually 110 μL of the solution was used for spin-coating at a speed of 3000 rpm for 30 seconds. Then in the further experiments, we also compared the performance of annealing the samples in the glovebox and annealing outside of the glovebox at 100℃ for 30 min in the hood.

2.5 Deposition of Perovskite Layer

Deposition of the absorber layer, that is, the perovskite layer in the PSCs is the most critical process step. The perovskite materials have been used for deposition by different methods such as spray pyrolysis (Barrows, Pearson et al. 2014), dip coating (Burschka, Pellet et al. 2013), chemical vapor deposition (Chen, Zhou et al. 2013), spin-coating (Lee, Teuscher et al. 2012), atomic layer deposition (Sutherland, Hoogland et al. 2015), and thermal evaporation (Malinkiewicz, Yella et al. 2014). In this thesis, we employed spin-coating for the perovskite layer, and we deposited the perovskite films in the N_2-filled glovebox with one-step spin-coating method.

In this method, all perovskite composition materials were mixed with a specific molar ratio and dissolved in a solvent such as DMF and DMSO or a mixture of them. Then, the solution was left on the stir with a temperature of 65℃ for a few hours until overnight in order to get a homogeneous solution. Then, the solution deposited on the SnO_2 layer samples with the anti-solvent method by spin-coating followed by annealing step. This method requires fewer fabrication steps compared to the two-step method. Many research articles reported the fabrication of high-efficiency PSCs using the one-step spin-coating method (Jeon, Noh et al. 2015, Roldan-Carmona, Bi, Yi et al. 2016, Saliba, Matsui et al. 2016). For example, Roldan et al. used a non-stoichiometric PbI_2:CH_3NH_3I ratio in the precursor solution and achieved a maximum PCE of above 19.09% (Roldan-Carmona, Gratia et al. 2015). Maximum efficiency of 20.8% was achieved with the one-step spin coating method from a solution containing a mixture of FAI, PbI2, MABr, and $PbBr_2$ (Bi, Tress et al. 2016). The molar ratio of 1.05 for PbI2/FAI was found to be critical in the preparation of the perovskite solution for this method (Bi, Tress et al. 2016). Saliba et al.

added a small amount of oxidation-stable rubidium cation (Rb^+) into the perovskite precursor solution with the one-step method which resulted in an efficiency of 21.6% on small active areas (Saliba, Matsui et al. 2016). This device also shows good stability characteristic under the full illumination and maximum power point tracking condition. In addition, in another work, Saliba et al. incorporated Cesium (Cs) into the perovskite precursor solution to own triple cations including FAI, MAI, and CsI (Saliba, Matsui et al. 2016). Using this technique with the one-step spin-coating, a stabilized power output of 21.17% are achieved. Also, Bi et al. used poly (methyl methacrylate) (PMMA) as a template to control the growth of perovskite crystals using the one-step fabrication method (Bi, Yi et al. 2016). With this approach, shiny and smooth perovskite films with excellent electronic properties fabricated, and maximum efficiency of 21.6% is reported (Bi, Yi et al. 2016). In this thesis, we used the one-step spin-coating with the anti-solvent method for fabrication of planer PSCs inside the glovebox. The Cs-doped mixed cation perovskite solution with a molarity of 1.3M and final formula of $Cs_{0.05}(MA_{0.15}FA_{0.85})_{0.95}Pb(I_{0.85}Br_{0.15})_3$ was usually used in this experiment.

2.6 Deposition of Hole Transport Layer

The hole transport layer (HTL) was deposited by using spin-coating a 70 mM solution of 2,2',7,7'-tetrakis-(N,N-di-p-methoxyphenylamine)9,9'-spirobifluorene (Spiro-OMeTAD) (purchased from Borun Chemicals Ltd, and Sigma Aldrich) in chlorobenzene (85.78mg/ml), with three additives to increase its conductivity. Spiro-OMeTAD is an organic p-type semiconductor that is typically mixed with other p-type dopants to improve its conductivity. Three dopants were usually used to dope the spiro-OMeTAD: 4tert-butylpyridine (4TBP), FK209 Co (III), and Li-TFSI. Based on our experiments, 4-

tert butylpyridine also aids the Li-TFSI solution to dissolve into the HTM solution readily. Without 4-tert-butylpyridine, the Li-TFSI dopant cannot get dissolved into the solution of spiro-OMeTAD in Chlorobenzene. If we add Li-TFSI dopant into the spiro-OMeTAD solution before the 4-tert-butylpyridine, a milky in color solution with large undissolved particles will form. Thus, 28.8µL of 4-tert-butylpyridine was added into the solution of spiro-OMeTAD in chlorobenzene (CBZ) firstly. Then, 17.5 µL from a solution of Li-TFSI in acetonitrile (520 mg/ml) was added to the HTM solution. At this step, the color of the solution is slightly yellow. Finally, 23µL of FK209 solution (150 mg/mL in acetonitrile) added to the HTM solution which changes the color of the whole solution into dark black upon addition. The molar ratio of dopants to the spiro-OMeTAD is 0.5, 0.03, and 3.3 for Li-TFSI, FK209, and 4TBP, respectively. After annealing of perovskite layer, samples left in glovebox (depends on the environment) for a few minutes to cool down until the room temperature. Then, 70 µL of HTM solution spin-coated on the samples at 4000 rpm for 30 seconds. No annealing step used at this step. Devices were then left overnight in the air and glovebox for the Spiro-OMeTAD to dope via oxidation. It should be mentioned that the HTM layer must cover all surface of the perovskite. Otherwise, the humidity will affect the perovskite layer during the oxidation process of spiro-OMeTAD in a dry box. Also, if HTM solution could not cover the perovskite surface completely, we used a swab wetted with DMF to remove the uncovered parts of the perovskite and to clean the edges of the substrate.

2.7 Deposition of Back Contact Gold Layer

In this thesis, the thermal evaporation is the most frequently used method for deposition of back contact in the PSCs, since it has cheap, easy, and short time advantages. By this

method, the source material was heated to a high temperature at high vacuum so that the material can evaporate toward the substrates.

For a common evaporation process, the samples and source material were carefully arranged and installed in the system. The distance from the filament to the crystal and the samples were carefully measured to calculate the tooling factor. The distance of the filament to the crystal sensor and samples was typically set to 12-15 cm. By this way, we make sure the samples will not become high temperature during evaporation. Then the chamber was pumped down for at least 45 minutes to reach to a vacuum of about 1x10-5 mbar. The filament heated up with increasing the voltage to start the deposition process. A pre-deposition of about 5-20 nm was used to clean the surface of source material and to make sure the deposition rate is stable. Then, 80 nm gold deposited at a low deposition rate of 0.5-1 A/sec. Finally, at the end of the deposition process, we left samples inside the chamber for 5-15 min to cool down and not get stress upon quick exposure to the room temperature. The rapid cooling of the samples might introduce cracks in the gold layer since the thermal expansion coefficients of the substrate and the gold are different from each other.

In this system, we used a straight coil filament for our experiments and could deposit the crack-free gold layer. Also, we need to clean the filament thoroughly and perform a high-rate pre-deposition step. Thus, we concluded that the quality of the gold layer gets affected by the type and cleanness of the filament. Therefore, the straight filament was helpful to get crack-free gold films. In this case, the filament including gold wire was cleaned with acetone, IPA, and DI water thoroughly. Then, a one-minute pre-heating step was used before starting the deposition of gold. In this way, we get rid of any

contaminations present on the filament. Therefore, with a suitable distance between samples and the filament, and a low deposition rate of 0.5-1 A/sec along with 10-15 min cooling down a step, we could make gold layers without cracks by using the thermal evaporator. In brief, to get a crack-free gold layer on the HTM layer, we advise that when using the filament for the first time, it is good choice to bake the filament at above 900 C for at least 10 min to remove the contaminations. Also, it is critical to clean the filament before use with acetone, IPA, and DI water, respectively. Moreover, the best crucible for deposition of gold by thermal evaporation is the alumina-coated crucibles since the gold is a refractory metal that can alloy with Tungsten in the regular basket filaments. Here we used the straight filament made of Tungsten to get a crack-free gold layer. The thermal deposition system is shown in Figure 2.6 below:

Figure 2.6 Thermal deposition system for gold electrode.

2.8 Current-Voltage Measurement

For this thesis, the J-V measurement systems in the Graham Research Lab of Department of Chemistry at the University of Kentucky were used. All solar cells masked with a metal aperture which was used to define the active area of the devices. Also, all measurements were performed in forward bias scan and reverse scan. Forward scan means sweeping voltage from the short circuit current toward the open circuit voltage. Reverse scan measurement means sweeping voltage from open circuit voltage toward short circuit current. This system is located inside the N_2-filled glovebox.

In this system, a SS150 solar simulator (Scientech) was calibrated to give simulated AM 1.5 sunlight at an irradiance of 100 mW/cm2. The irradiance was calibrated using an NREL-calibrated KG5 filtered silicon reference cell. Current-voltage curves were recorded by a source meter (Keithley).

Thus, the results provided in Chapter 3 were measured with this system. The J-V measurement system is shown in the graph below:

Figure 2.7 The main components of J-V measurement system.

2.9 Scanning Electron Microscopy (SEM)

SEM is one of the most regularly used microscopy techniques in material structure analysis. In this thesis, we used Quanta 250 environmental scanning electron microscopy (ESEM) with energy dispersive spectroscopy (EDS/EDX). The Quanta 250 environmental SEM was also employed to obtain the surface images of samples.

CHAPTER 3. RESULTS AND DISCUSSION FOR PEROVSKITE SOLAR CELLS PROCESSED IN GLOVEBOX ENVIRONMENT

Some high performance perovskite solar cells are fabricated in the environmentally controlled, N_2-filled glovebox system. In these systems, humidity is less than one parts per million (ppm). Therefore, the perovskite films will not be affected by the moisture. Also, a one user two-handed N_2-filled MBraun glovebox with a varying pressure from three to six mbar was used for fabrication of perovskite solar cells. Besides, we had FTO coated glass (Pilkington, 8 $\Omega.cm^{-2}$) as the substrate in this chapter. This substrate provides high conductivity with transmission above 76%. It is an excellent choice for applications since low series resistance is required. Thus, the experiments we conducted in this thesis followed the procedures: cleaning FTO substrates, deposition of SnO_2 electron transport layer deposition of perovskite layer using spinning coater. Finally, a thermal evaporator was used for deposition of gold as the back contact. The J-V measurements were performed in the measurement system placed inside a glovebox in Graham lab at Chemistry Department.

3.1 Brief history for Perovskite Solar Cells Processed in N_2-filled Glovebox Environment

Recently, PSCs have been proved that the PCEs to be larger than most organic solar cells, comparable to those of commercialized silicon solar cells and others based on inorganic semiconductors. The efficiency of PSCs reaches 24.2% in 2019, which initially started from a value of 4% in 2009. Currently there are many reports on high efficiency PSCs. For example, Jeon et al. incorporated Bromide (Br) into perovskite in order increase the band gap of perovskite materials, and thus increase the open circuit voltage of the device

to get high efficiency (Jeon, Noh et al. 2015). Moreover, incorporation of Br into the perovskite stabilized the perovskite layer against humidity degradation. In this work, a bilayer architecture of PSC from a combination of $MAPbBr_3$ and $FAPbI_3$ displays an average efficiency of 16.2% with a maximum efficiency of 18.5% (Jeon, Noh et al. 2015). Ahn et al. fabricated highly compact perovskite layers by the spin-coating of a solution of methylamine, lead iodide, DMF, and DMSO, along with using diethyl ether as anti-solvent to remove DMF during spin-coating. Via this technique, the authors reported stable and highly-reproducible PSCs with an average efficiency of 18.3% for 41 cells. The best PCE of 19.71% obtained by this method (Ahn, Son et al. 2015). A high-efficiency PSC reported by Yang et al. with a new fabrication technique named as intermolecular exchange method (Yang, Noh et al. 2015). This method offers full conversion of PbI_2 for perovskite. Besides, it creates large and flat grain size perovskites, which are critical to reduce the number of defects. Also, the perovskite layer with flat surface offers a smooth substrate for deposition of a thin HTM layer on top of the perovskite layer. Therefore, PSCs fabricated with this method presented a maximum efficiency of 20.1% with an average efficiency of over 19% (Yang, Noh et al. 2015).

Yi et al. reported efficiency of 20.75% for PSCs fabricated by two-step spin-coating method (Yi, Li et al. 2016). They worked on the complete conversion of the mesoporous PbX_2 precursor to perovskite with a mixed solution of $PbBr_2$, MABr, FAI, and PbI_2 in a mixed solvent including DMF and DMSO (Yi, Li et al. 2016). The main point of Yi et al.'s work is making an excellent infiltration of perovskite into a mesoporous PbI_2 layer by the reagent solution. In another research, Bi et al. have reported a new metal halide PSCs with maximum efficiency of 20.8% fabricated in the glovebox by one-step spin-

coating method (Bi, Tress et al. 2016). This new perovskite with formula $MAFAPbI_xBr_{(1-x)}$ consists of a mixture of FAI, PbI_2, MABr, and $PbBr_2$ with the precisely controlled composition of materials. The PbI_2/FAI molar ratio of 1.05 in the precursor solution is an important parameter in order to have highly-efficient PSCs (Bi, Tress et al. 2016). Crystallization of perovskite is the most challenge part in the fabrication of PSCs, since defects such as pinholes and grain boundaries mostly develop during this step. In work reported by Bi et al., a new approach was introduced to prepare high-quality perovskite films using poly (methyl methacrylate) (PMMA) as a template. PSCs fabricated by this approach display a certified efficiency of 21.02% and a maximum efficiency of 21.6% with an open-circuit voltage of 1.14 V, short-circuit current of 23.7 mA/cm^2, and fill factor of 78% (Bi, Yi et al. 2016). In another work, Saliba et al. reported incorporation of small and oxidation-stable rubidium cation (Rb^+) into perovskite materials. PSCs fabricated by this technique shows a stabilized efficiency of 21.6% with an average efficiency of 20.2% (Saliba, Matsui et al. 2016). It suggests that a 5% incorporation of Rb^+ is the optimal value to get the best performance PSCs (Saliba, Matsui et al. 2016). Finally, Yang et al. recorded the highest efficiency for PSCs by the introduction of additional iodide ions into the organic cation solution with two-step spin-coating method through the intermolecular exchange process. The best efficiency of 22.6% with a certified efficiency of 22.1% is reported (Yang, Park et al. 2017).

3.2 SnO_2 as the Electron Transport Layer in the PSCs

As a high performance solar cell, the energy levels of various materials must be well aligned. For example, the band gap in the light absorber must be appropriate for absorbing visible light. Also, the conduction band edge in the light absorber should be slightly higher than the conduction band edge of the n-type semiconductor, and then electrons can be efficiently injected from the light absorber to the ETL. Interestingly, all of these energy levels can be altered with different ways. For example, by changing materials for the carrier transport, the conduction band edge will also change. Stability and scalability have become the two main challenges for perovskite solar cells with the research focus in the field advancing toward commercialization. Charge transport layers are found to be critical for device performance and stability. A traditional electron transport layer (ETL), such as TiO_2, is not very efficient for charge extraction at the interface, especially in planar structure. In addition, the devices using TiO_2 suffer from serious degradation under ultraviolet illumination.

Compared with TiO_2, SnO_2 possesses several advantages such as higher mobility and better energy level alignment. More importantly, using of SnO_2 as ETL can eliminate/minimize degradation of perovskite solar cells induced by TiO_2 as ETL, leading to significantly enhanced operational lifetime under continuous light illumination. Besides, in contrast with TiO_2, SnO_2 could be easily coated by low temperature solution process, electrodeposition process, atomic layer deposition, chemical bath deposition, electron-beam deposition, and sputtering deposition.

SnO_2 has attracted great attentions as ETL for PSCs, and it is considered as the most promising alternative to TiO_2 due to following reasons: 1) SnO_2 owns deep conduction

band and good energy. 2) SnO_2 owns high bulk electron mobility of up to 240 cm2 V-1s-1 and high conductivity, which can potentially improve the electron transport efficiency and reduce the recommendation loss. 3) SnO_2 has wide optical bandgap and high transmittance over the whole visible spectra. 4) SnO_2 is easily processed by low temperature methods (<200℃). 5) SnO_2 showed excellent chemical stability, UV-resistance properties, and less photocatalytic activity in comparison with TiO_2 or other ETLs, which is helpful for overall device stability (Qi Jiang et. al. Small, 2018).

3.2.1 Sputtered the SnO_2 thin film by sputtering system

Here we used the sputtering to sputter the SnO_2 film, and the thickness of the layer was controlled by some factors such as power, deposition rate, and the deposition time. The SnO_2 target had a purity of 99.99%, and the distance between the target and sample was about 10 cm. The chamber was pumped down for 75 min to get the pressure of 0.05 mTorr. To clean the target surface, the pre-deposition process performed for 6 min or 150 °A. The process was completed in pure Ar gas with a flow meter of 15 sccm (standard cubic centimeter per minute). The sputtering process of compact SnO_2 was finished at the power of 150W with a deposition rate of 0.7 °A/sec at a working pressure of 4.1 mTorr. In the case of gold sputtering, the power was 16 W to have a deposition rate of 0.5 °A/sec at a pressure of 3.6 mTorr. The film thickness was adjusted by the sputtering time and monitored by the film thickness meter which was mounted on the substrate stage in the chamber. After depositing SnO_2 electron layer, we do the same steps in the following procedure as the solution process method. Then we measured the PCE by J-V measurement system, which is shown in the graphs below. From the graph, we can see

that the reverse PCE is only 7.56%, and forward PCE is only 4.28%. Also, the fill factor is very lower than normal one. We have tried to change the thickness of SnO_2, and changed the annealing temperature, but the results are almost same. After reviewing some literature, we found that it needs 90% percent oxygen and 10% Ar instead of 100% Ar when sputtered the SnO_2 film. Due to lacking enough oxygen, we stopped using sputtering SnO_2 method, and switched to use solution process method for the further experiments.

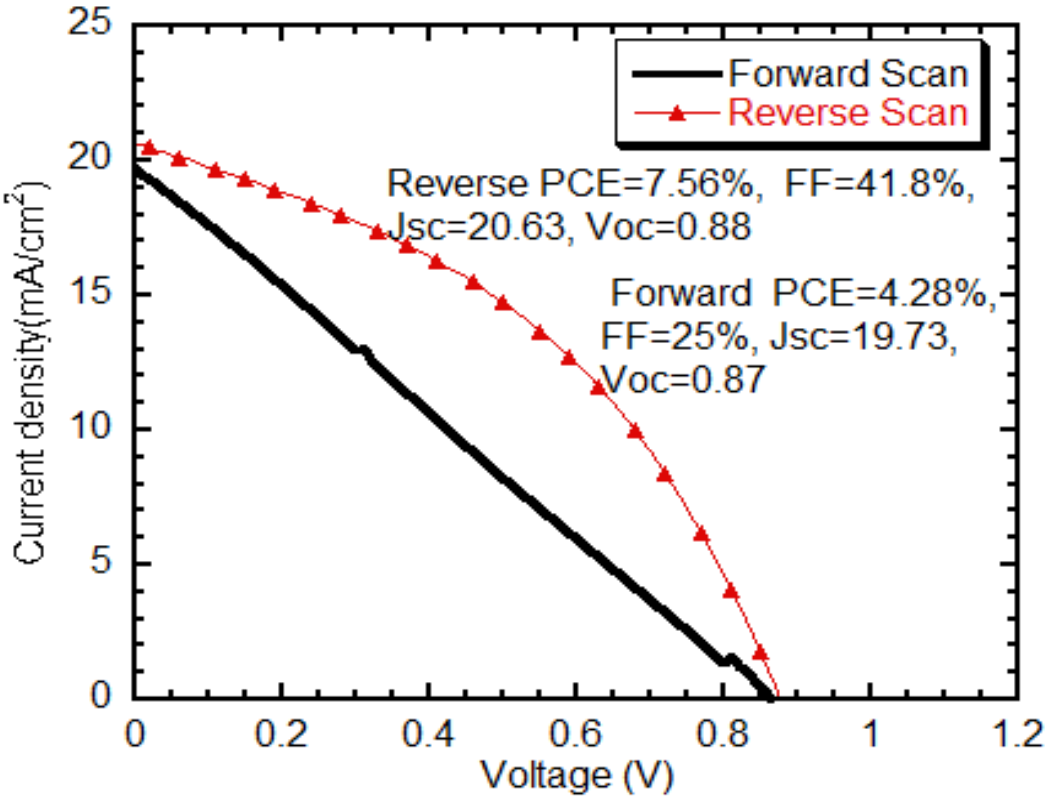

Figure 3.1 Performance of devices using sputtering SnO_2 film.

3.2.2 Annealing outside or annealing in the glovebox after deposition of electron transport layer by solution process method

In our experiments, we wanted to test the question: should we do the thermal annealing in ambient air, or do the thermal annealing in the glovebox? Thus, we design the experiments below: we bought $SnCl_4$ (99.995%) from sigma, and the concentration is 2.226g/mL. Here we add 50μL $SnCl_4$ in 4.275 mL ethanol as the solution. Then we deposited 95μL solution for each substrates. For substrates 7 and 1, we did the annealing for 0.5 hour in the glovebox; for sample 8 and 4, we did annealing for 0.5 outside the glovebox. Also, we finished the same procedures for all the samples. Then we tested the performance of each samples. The graph (a) represents the sample 4, which is done the annealing outside of the glovebox. The graph (b) represents the sample 8, which is done the annealing in the glovebox. From the power conversion efficiency of these two samples, we can conclude that annealing the samples outside the glovebox is better than annealing the samples inside the glovebox. We think that the oxygen outside the glovebox is much more than the oxygen inside the glovebox, and the $SnCl_4$ on the substrates can better converted into SnO_2 due to the efficient oxygen outside the glovebox.

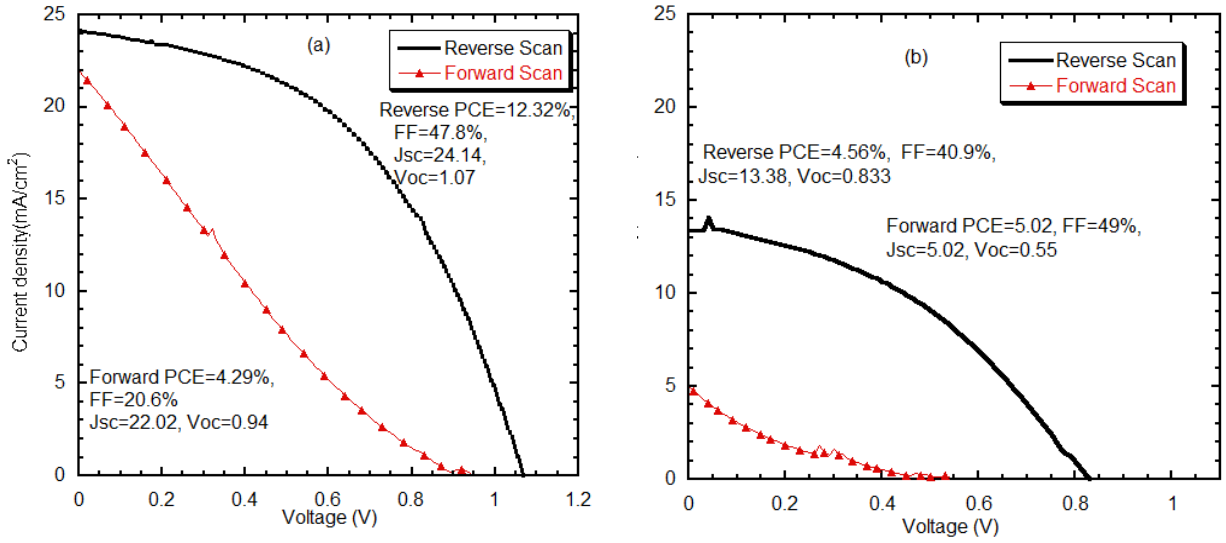

Figure 3.2 Comparison of perovskite solar cells performance annealed inside the glovebox and outside the glovebox.

3.3 Cesium-Doped Mixed Cation PSCs

Although $FAPbI_3$ has lower band gap compared to the $MAPbI_3$ perovskite with a band gap of 1.55 eV, $FAPbI_3$ is not stable at the room temperature (Stoumpos, Malliakas et al. 2013, Lee, Seol et al. 2014, Jeon, Noh et al. 2015). The best PSCs reported by now are from mixed cation perovskites containing both MA and FA, but these perovskites are thermally unstable and sensitive to the processing method. Doping perovskite with Cesium is a pathway to keep the whole material stable. Therefore, Saliba et al. suggested the mixed cation perovskite doped with Cesium with a general formula of $Cs_x(MA_{0.17}FA_{0.83})_{(100-x)}Pb(I_{0.83}Br_{0.17})_3$ (Saliba, Matsui et al. 2016). They reported the fabrication of high efficiency and highly-reproducible PSCs by the Cs-doped mixed cation perovskites. In this chapter, we focused on the fabrication of Cesium-doped mixed cation PSCs in the glovebox and optimized several parameters to increase the efficiency of PSCs in our lab. For the fabrication of PSCs in the glovebox, we mainly conducted the

experiments according to the following procedures: Firstly for the SnO_2 electron transport layer deposition, then the perovskite layer deposition, next we deposit the hole transport layer, and the last step we finish the electrode deposition. In detail, the samples were left on the hotplate with a temperature of 100°C for the annealing process after electron transport layer finished. In this way, the moisture would not affect the surface of the samples. Later on, when deposition of perovskite and HTM completed, we cleaned the FTO area with a blade to remove the perovskite layer, and then a swab wetted with DMF and ethanol. At first we used the Kapton tape to cover the FTO part in our experiments, but after some experiments, we found that the Kapton tape leaves some residue on the surface of FTO. Besides, Kapton tape prevents the uniform distribution of the perovskite solution during spin-coating, especially for the anti-solvent method. Also, when we set the stir's temperature to 65°C, the solution is divided into two separate liquid regions with different densities. Thus, after an overnight stirring, we decrease the temperature of the stir to 45°C a few hours before deposition of perovskite to have a homogenous solution.

3.4 Fabrication and Optimization of Cs-doped Mixed Cation Perovskite

In this section, we summarized the processing issues we solved during fabrication of the perovskite film in the glovebox. Dryness of the glovebox and the spin coater environment plays a vital role in getting a high-quality perovskite film. In literature, the one-step spin-coating using the anti-solvent method with the spin-coating speed at 1000 rpm for at least 10s followed by spin-coating at high-speed was usually used for deposition of the perovskite layer. Nevertheless, it does not work for our fabrication setup. The perovskite film will get dry quickly during the first spin step at 1000 rpm due to open-cap spin-

coater. Thus, the 10 s spinning at low speed does not provide a shiny, black, and smooth surface perovskite layer. Therefore, we optimized the spin-coating parameters to 1000 rpm for 10 sec followed by 4000 rpm for 30 secs to get a decent perovskite film. A 100 µL of CBZ is dropped on the substrates after 20s during the second spin step at 4000 rpm.

3.5 Different Concentrations of SnO_2 Solution for Electron Transport Layer

Here we tried different concentrations of SnO_2 as the Electron Transport Layer, since in the literature, one is said 20% in H_2O colloidal dispersion, and the other said the accurate concentration is 15%. So here we use two kinds of SnO_2 solution. For solution 1, we mixed 267µL of SnO_2 mixed with 1730 µL of water as the concentration of 20%. For solution 2, we mixed 333µL of SnO_2 mixed with 1670 µL of water as the concentration of 15%. Then we tested the performance of Perovskite Solar Cells by Current-Voltage Measurement. For the graph (a), it expressed the test results of perovskite solar cells, which use the solution 1 (20%) as the SnO_2 electron transport layer. For the graph (b), it shows the test results of perovskite solar cells, which use the solution 2(15%) as the SnO_2 electron transport layer. From the tests results, we can find that the performance of perovskite solar cells that use the 20% SnO_2 solution is better than the performance of perovskite solar cells that use the 15% SnO_2 solution. Thus, in our further experiments, we will use the 20% SnO_2 solution for the electron transport layer deposition.

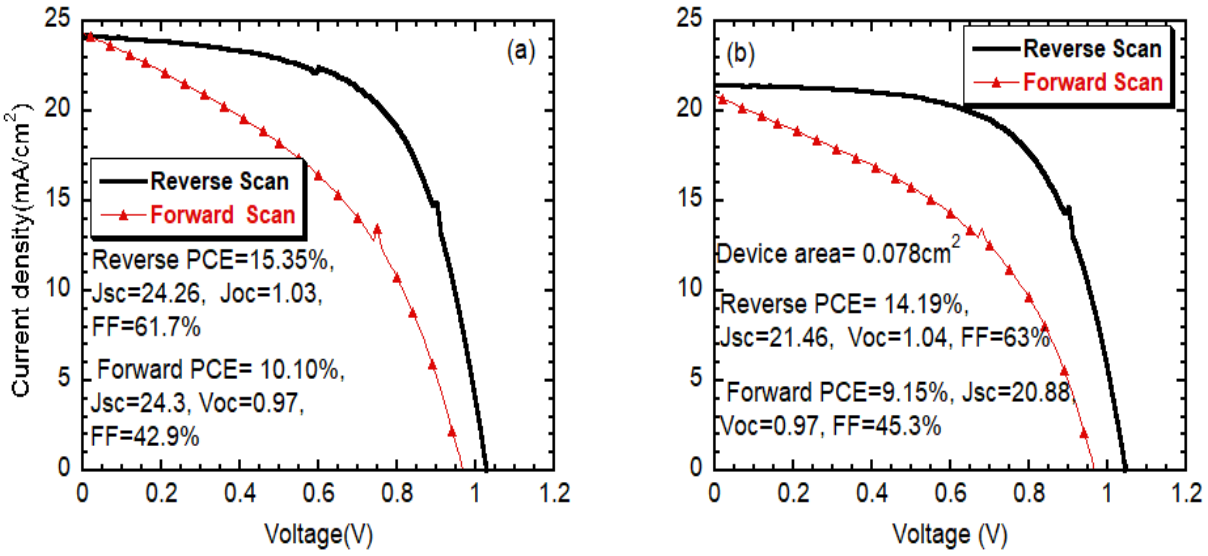

Figure 3.3 Comparison of perovskite solar cells performance which are deposited with different concentration of SnO_2.

3.6 Keeping the SnO_2 layer on the electrode instead of scratching

After deposition of Gold layer as the electrode, we usually scratch some electron transport layer on the substrates, in order to expose the electrode. However, in our experiments, we do not scratch the electron transport layer SnO_2, and the samples work well when we do the Current-Voltage Measurement. From the paper we checked, we find that the band gap value of SnO_2 is about 3.7 eV. For the band gap value of FTO (Fluorine-doped tin oxide) is about 3.8 eV. Thus, the band gap value of SnO_2 and FTO is almost the same, and the electrons can be easily transported between SnO_2 layer and FTO substrate.

3.7 Using filter for Perovskite solution

In order to block big perovskite particle and get high quality perovskite solution, we used filter for the perovskite solution, and then deposited on the substrates. In detail, we filtered the perovskite solution (PTFE filter with pore size of 0.45μL was used) before the deposition of the perovskite. This step is critical for getting a smooth and shiny perovskite film. Otherwise, there will be some particles in the solution which are not dissolved completely, making the surface of perovskite non-smooth. The solution is prepared inside the glovebox. Also, we dropped the perovskite solution at different angle such as 70 degree, 45 degree and so on. Here we deposited perovskite solution on 8 substrates. We used 150 μL perovskite solution, 100μL CBZ for each sample. For sample 1, we adopted 1000 rpm 10sec and followed by 4000 rpm, 30sec, 45 degree. For sample 2, we adopted we adopted 1000 rpm 10sec and followed by 4000 rpm, 30sec, 80 degree. For sample 3,4,5, 7, we adopted 1000 rpm 10sec and followed by 4000 rpm, 30sec, 70 degree. When deposited for sample 4, 7, we used slow drop like two drops. For the Sample 5, we dropped the solution too fast. For sample 6,8 we adopted 1000 rpm 10sec and followed by 4000 rpm, 45sec, 70 degree. We used current-voltage measurement to test the samples, and we got the results below. For the sample 3, we get the best result: the reverse scan PCE is18.13%, and the forward scan PCE is 15.49%. Thus, the difference between reverse scan PCE and forward scan PCE is smaller than before, so using filter is helpful to reduce the hysteresis.

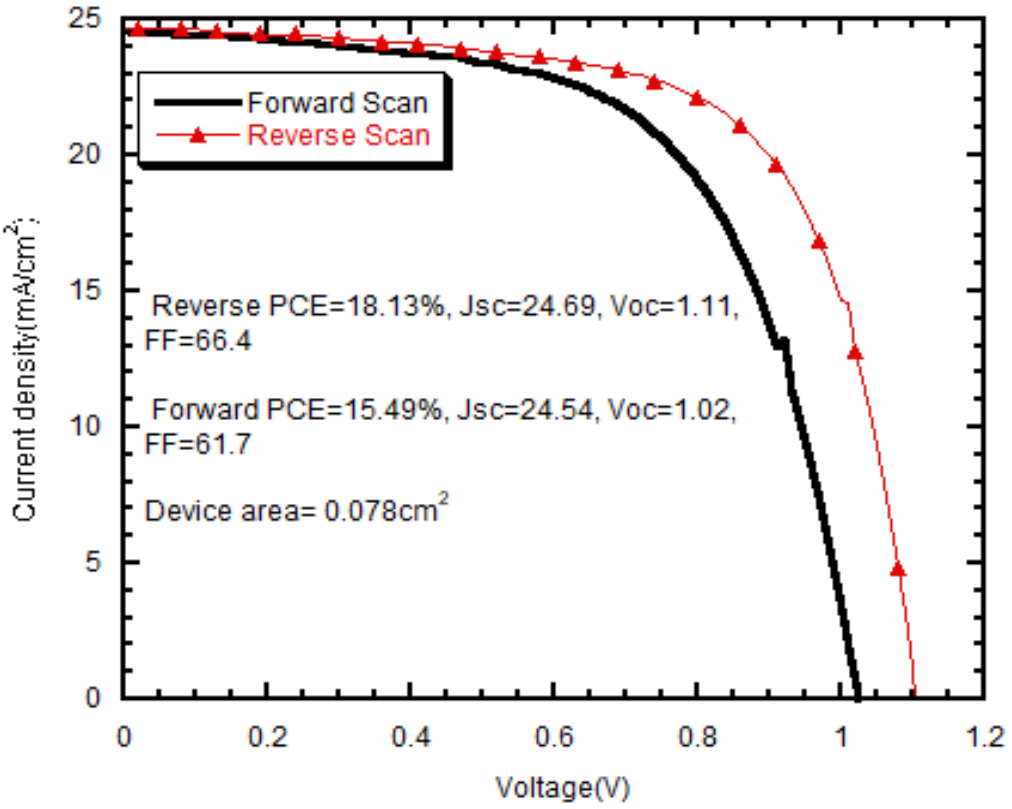

Figure 3.4 J-V curve of the best device in small size (0.078 cm^2) measured from reverse and forward scan under one-sun condition (AM 1.5G, 100Mw cm^{-2}).

3.8 The dropping chlorobenzene solution angle impact on the performance of the samples

Here we use the same experiment parameters except different dropping chlorobenzene solution angles. We compared the performance of samples with 45 degrees and 70 degrees, and we get the PCE of the samples shown in the graphs. From the Current-Voltage measurement, we get that the PCE of samples that are dropped chlorobenzene at 70 degrees is better that the PCE of samples that are dropped chlorobenzene at 45 degrees. We think that the chlorobenzene solution can be deposited uniformly when dropped at 70 degrees.

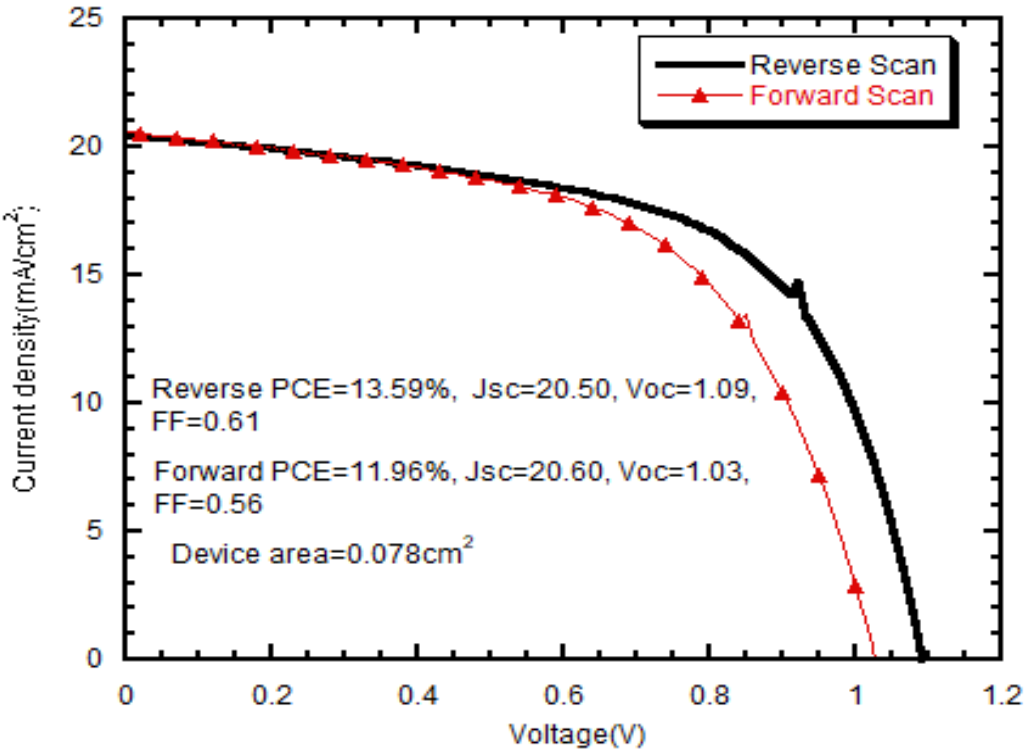

Figure 3.5 J-V curve of the device that is dropped solution at 45 degree in small size (0.078 cm^2) measured from reverse and forward scan under one-sun condition(AM 1.5G, 100Mw cm^{-2}).

3.9 Using filter for both Perovskite and Hole transport layer solution

Here we also use filter for the HTM solution beside PSK solution, and we keep the experiments parameters the same as the last experiments except using filter for PSK solution and HTM solution. Also, we used current-voltage measurement system to evaluate the performance of the samples.

From the measurement, we find that the PCE is lower than that before. Thus, using filter for PSK solution and HTM solution together is not as good as using filter only for PSK solution. We think that the HTM layer became thinner than before the filter was used, and that is not good for entire performance of Perovskite Solar Cells.

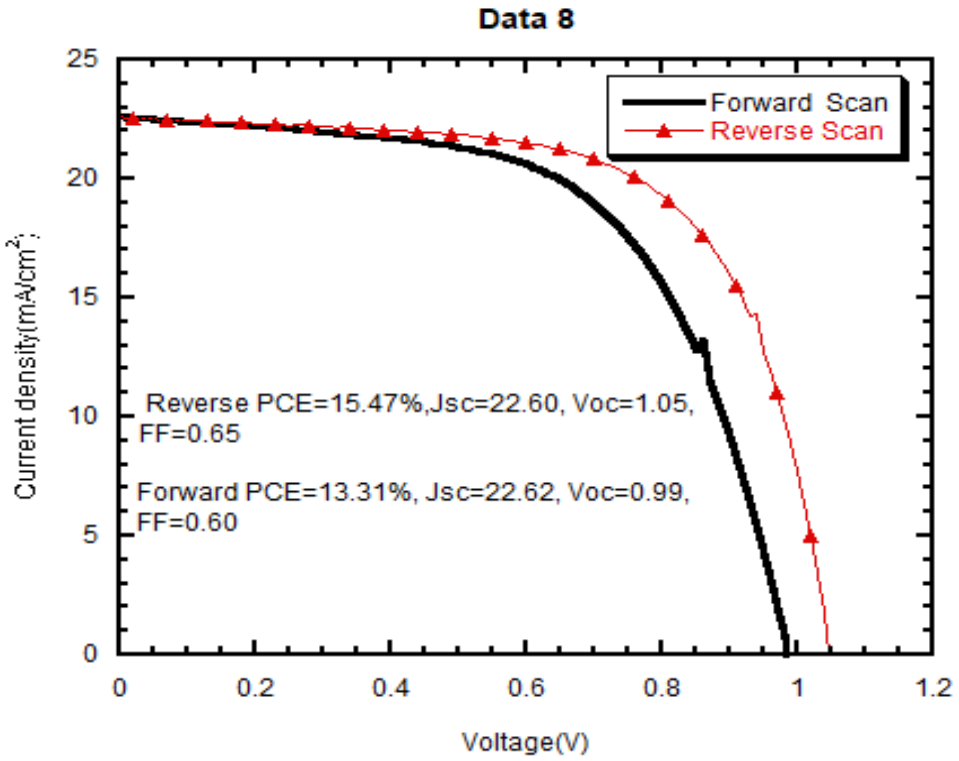

Figure 3.6 The best performance of perovskite solar cells after filter of perovskite solution and HTM solution.

3.10 Perovskite Solar Cells without SnO_2 electron transport layer

Since the band gap of SnO_2 is about 3.7 eV. , the band gap value of FTO (Fluorine-doped tin oxide) is about 3.8 eV. Thus, the band gap value of SnO_2 and FTO is almost the same. Then we designed an architecture without SnO_2 electron transport layer, and tested the performance by current-voltage measurement. From the graph, we can see that the performance of perovskite solar cells without SnO_2 electron transport layer is much worse that with SnO_2 electron transport layer. We think that the quality of FTO is not good enough compared with the quality of the SnO_2 layer we deposited, since it is fabricated by conventional factories.

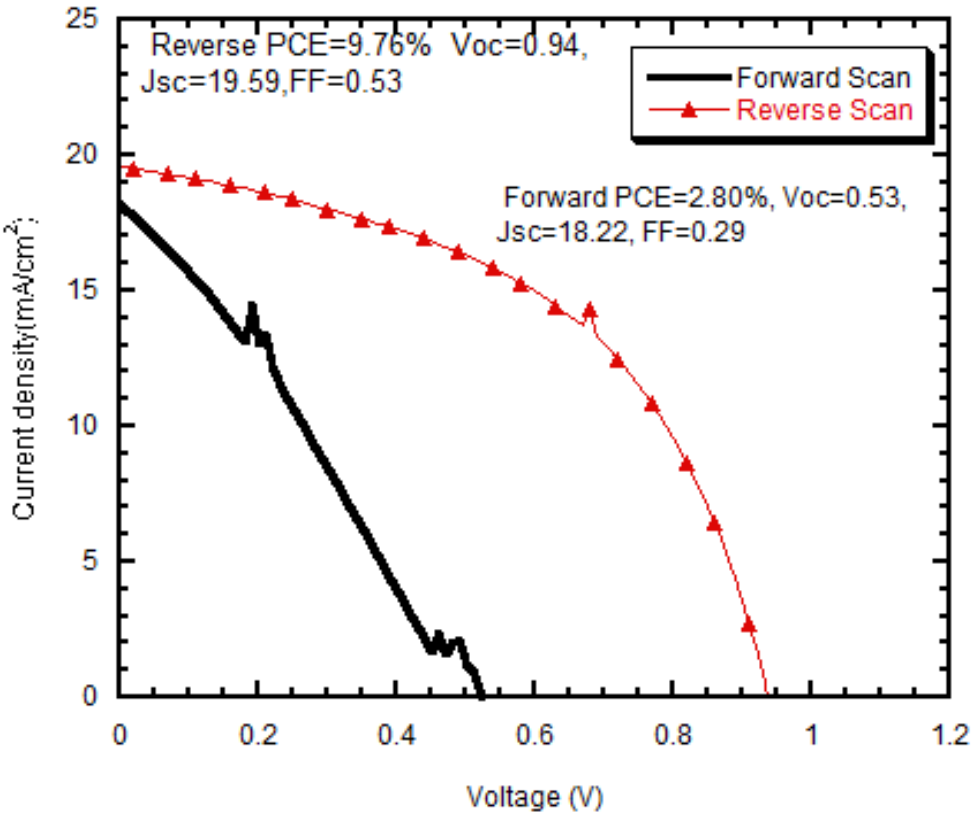

Figure 3.7 The performance of perovskite solar cells without SnO2 electron transport layer.

3.11 Back Contact Electrode

Gold was usually used as the back electrode in the PSCs. We mainly used the thermal evaporation methods for deposition of the gold layer for PSC fabricated in the glovebox. In this section, we studied the crack on the surface of the film, and tried to solve this problem.

The gold layer suffers from large cracks in the size of 300-500 nm if we use thermal evaporation. These cracks deteriorate the performance of the devices in many ways. Firstly, the cracked film may ineffectively collect the holes from the HTM layer owing to not strong adhesion to the HTM layer. Secondly, the cracks inside the gold layer reduce

the actual active area of the device, and thus underestimate the real device area. Thirdly, the cracks inside the gold layer can provide a pathway for the moisture to contact the HTM layer and affect the stability of the devices. We tried both spiro-OMeTAD and CuSCN HTMs to test the above parameters and found the cracks in the gold layer do not come from the substrate, thermal deposition rate, distance between source and samples, and the process of cooling. The cracks were still in the layers for all cases. Also, we should mention that our samples were exposed to the humidity for 1-2 hours before deposition of the gold and measurement of the cells. Figure 3 shows the top-view SEM image of the gold layer deposited by thermal evaporation. The cracks are present in the Au film according to the cross-sectional image. Thus, the active area is not accurately defined by the gold layer. The gold layer with such large cracks cannot prevent humidity from contacting the HTM layer. Although the overnight oxidation of HTM film is essential for high-performance PSCs, long-term exposure to the humidity damages the HTM film and deteriorates the overall performance of the device In order to make a crack-free Au layer on the HTM, we need to use the suitable crucible (straight coil and alumina-coated basket filament), then clean it with solvents and DI water thoroughly to not have any contamination on the filament and gold residue. Also, a pre-deposition step at high temperature is highly advisable before starting the deposition of gold. Besides, we used Tungsten basket crucible for deposition of Au. However, it always cause a full crack gold film. Finally, we found that a straight filament along with a cleaning process can make a crack-free gold layer.

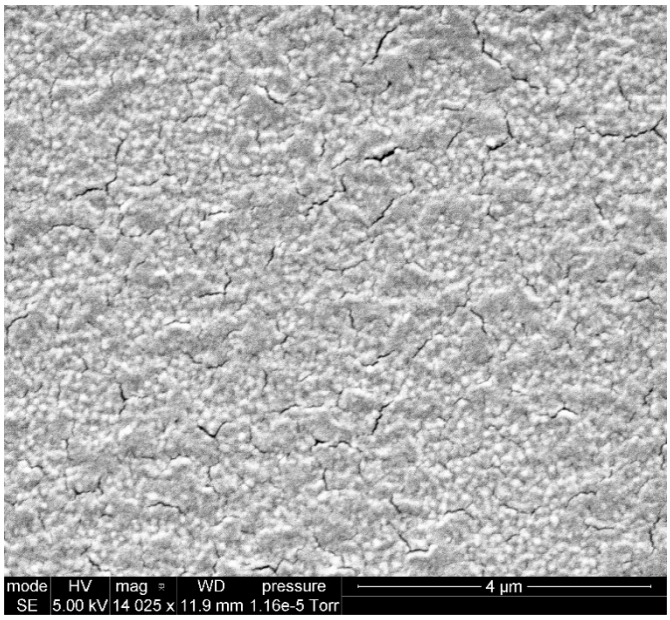

Figure 3.8 Crack on the surface of Gold Electrode by SEM.

CHAPTER 4. CONCLUCTION AND FUTURE WORK

4.1 Conclusion

PSCs have demonstrated the PCEs greater than organic solar cells and comparable to those of commercialized silicon solar cells. The PCE increased from 6.5 % in 2011 to beyond 24.2 % in 2019. The light absorber of the PSCs is a film made of $APbX_3$ ($A=CH_3NH_3$, $(NH_2)_2CH_2$ or Cs, X= I, Br or Cl). PSCs are considered as the most promising replacement of silicon solar cells due to their high efficiency at low manufacturing cost.

In this thesis, compared to using the conventional TiO_2 as the electron transport layer, we adopted SnO_2 as the electron transport layer, and we successfully fabricated perovskite solar cells with planer structure in the N2-filled glovebox environments. Also, we studied the impact of several parameters on the performance of PSCs with fabrication in the N_2-filled glovebox environments, such as the annealing environment impact, different concertation solution impact, using filter for the perovskite solution and HTM solution, the dropping angle of perovskite solution, keeping the SnO_2 layer instead of scratching, fabrication of PSCs without SnO_2 electron transport layer, and fill factor issue. Here, we addressed several issues with the methods regarding the substrate cleaning procedure, and the deposition of metal back contact without cracks by thermal evaporation. Finally, we fabricated PSCs with efficiencies as high as ~18.13% by spin-coating a cesium-doped mixed cation perovskite with the final formula of $Cs_{0.05}(MA_{0.15}FA_{0.85})_{0.95}Pb(I_{0.85}Br_{0.15})_3$ using the anti-solvent method. We believe the efficiency can be improved by new tests since some parameters such as the quality of substrates can be optimized in the further experiments.

4.2 Future Work

Although perovskites show excellent properties and PSCs recorded efficiencies higher than current commercialized CIGS solar cells, some issues still need more investigation for commercialization purposes such as the stability and hysteresis. A PV device need be flexible and lightweight for use in applications such as portable power sources and wearable products. In this case, low-cost roll-to-roll processing steps can be utilized.

Thus, fabrication of the PSCs on the flexible substrate is a topic for researchers. Currently, most high-efficiency PSCs have lead in their perovskite precursor. As lead is a toxic material and may cause an environmental hazard, which is harmful to human health. Therefore, it is important to investigate a low-cost and environmentally benign lead-free materials for perovskite solar cells, such as replacement lead with tin (Sn). The maximum efficiency of lead-free PSCs is lower than that of lead-based PSCs. Thus, further research on lead-free PSCs is needed. Also, MAI and FAI perovskites are sensitive to the moisture, and then the performance of the PSCs employing these perovskites degrade over time in high-humidity conditions. Therefore, encapsulation of the PSCs needs to be considered. In addition, the spiro-OMeTAD with additives such as Li-TFSI are sensitive to preparation, operation, and storage. Also, they are expensive compared to the other materials in the PSC. Thus, some other low-cost organic HTMs materials are needed that function as good as spiro-OMeTAD without additives. Moreover, the gold material for electrode in the PSCs is expensive too, and reducing the cost of the PSCs for commercialization is important. Therefore, it is important to increase the efficiency of PSCs and to investigate low-cost materials with excellent long term stability. For example, carbon is not sensitive to the humidity and shows excellent

adhesion to the HTM film. Thus, the replacement of Au with carbon paste and carbon nanotube as the back electrode can be investigated for the low-cost and large-scale production of PSCs. Moreover, the J-V measurement of PSCs demonstrates hysteresis in forward and reverse scan direction. At present, there are four primary mechanisms reported for explaining the J−V hysteresis behavior: (a) slow transient capacitive current, (b) dynamic trapping and de-trapping processes of charge carriers, (c) band bending due to ion migration, and (d) band bending due to ferroelectric polarization (Chen, Yang et al. 2016). For the main reasons, we need to investigate deeper in the further research. Furthermore, based our experiments and J-V measurements, current density and voltage for the devices are good, but the fill factors need to be improved. Thus, in the future work, improving the fill factor of the devices is one topic for further experiments.

BIBLIOGRAPHY

A.J. Nozik, R.Memming, J.Phys. Chem.1996,100 13061.

Burschka, J., N. Pellet, S.-J. Moon, R. Humphry-Baker, P. Gao, M. K. Nazeeruddin and M. Grätzel (2013). "Sequential deposition as a route to high-performance perovskitesensitized solar cells." Nature 499(7458): 316-319.

Cao, D. H., C. C. Stoumpos, C. D. Malliakas, M. J. Katz, O. K. Farha, J. T. Hupp and M. G. Kanatzidis (2014). "Remnant PbI2, an unforeseen necessity in high-efficiency hybrid perovskite-based solar cells? a)." Apl Materials 2(9): 091101.

Cappel, U. B., T. Daeneke and U. Bach (2012). "Oxygen-induced doping of spiroMeOTAD in solid-state dye-sensitized solar cells and its impact on device performance." Nano letters 12(9): 4925-4931.

Chen, Q., H. Zhou, Z. Hong, S. Luo, H.-S. Duan, H.-H. Wang, Y. Liu, G. Li and Y. Yang (2013). "Planar heterojunction perovskite solar cells via vapor-assisted solution process." Journal of the American Chemical Society 136(2): 622-625.

Eperon, G. E., S. D. Stranks, C. Menelaou, M. B. Johnston, L. M. Herz and H. J. Snaith (2014). "Formamidinium lead trihalide: a broadly tunable perovskite for efficient planar heterojunction solar cells." Energy & Environmental Science 7(3): 982-988.

Ibn-Mohammed, T.; Koh, S. C. L.; Reaney, I. M.; Acquaye, A.; Schileo, G.; Mustapha, K. B.; Greenough, R. Perovskite solar cells: An integrated hybrid lifecycle assessment and review in comparison with other photovoltaic technologies. Renewable Sustainable Energy Rev. 2017, 80, 1321−1344.

Im, J.-H., H.-S. Kim and N.-G. Park (2014). "Morphology-photovoltaic property correlation in perovskite solar cells: One-step versus two-step deposition of CH3NH3PbI3." Apl Materials 2(8): 081510.

Im, J.-H., C.-R. Lee, J.-W. Lee, S.-W. Park and N.-G. Park (2011). "6.5% efficient perovskite quantum-dot-sensitized solar cell." Nanoscale 3(10): 4088-4093.

Goldschmidt, V. M. (1926). "Die gesetze der krystallochemie." Naturwissenschaften 14(21): 477-485.

Grätzel, M. (2014). "The light and shade of perovskite solar cells." Nature materials 13(9): 838.

Green, M. A., K. Emery, Y. Hishikawa and W. Warta (2011). "Solar cell efficiency tables (version 37)." Progress in photovoltaics: research and applications 19(1): 84-92.

Hawash, Z., L. K. Ono and Y. Qi (2016). "Moisture and Oxygen Enhance Conductivity of LiTFSI‐Doped Spiro‐MeOTAD Hole Transport Layer in Perovskite Solar Cells." Advanced Materials Interfaces 3(13).

Heo, J. H., S. H. Im, J. H. Noh, T. N. Mandal, C.-S. Lim, J. A. Chang, Y. H. Lee, H.-j. Kim, A. Sarkar and M. K. Nazeeruddin (2013). "Efficient inorganic–organic hybrid heterojunction solar cells containing perovskite compound and polymeric hole conductors." Nature photonics 7(6): 486.

Helander, M. G., M. Greiner, Z. Wang, W. Tang and Z. Lu (2011). "Work function of fluorine doped tin oxide." Journal of Vacuum Science & Technology A: Vacuum, Surfaces, and Films 29(1): 011019.

Im, J.-H., H.-S. Kim and N.-G. Park (2014). "Morphology-photovoltaic property correlation in perovskite solar cells: One-step versus two-step deposition of CH3NH3PbI3." Apl Materials 2(8): 081510.

Jeon, N. J., J. H. Noh, Y. C. Kim, W. S. Yang, S. Ryu and S. I. Seok (2014). "Solvent engineering for high-performance inorganic–organic hybrid perovskite solar cells." Nature materials 13(9): 897.

Kearns, D. and M. Calvin (1958). "Photovoltaic effect and photoconductivity in laminated
organic systems." The Journal of chemical physics 29(4): 950-951.

Kim, H.-S., C.-R. Lee, J.-H. Im, K.-B. Lee, T. Moehl, A. Marchioro, S.-J. Moon, R. Humphry-Baker, J.-H. Yum and J. E. Moser (2012). "Lead iodide perovskite sensitized allsolid-state submicron thin film mesoscopic solar cell with efficiency exceeding 9%." Scientific reports 2: 591.

Kojima, A., K. Teshima, Y. Shirai and T. Miyasaka (2009). "Organometal halide perovskites as visible-light sensitizers for photovoltaic cells." Journal of the American Chemical Society 131(17): 6050-6051.

Lee, M. M., J. Teuscher, T. Miyasaka, T. N. Murakami and H. J. Snaith (2012). "Efficient hybrid solar cells based on meso-superstructured organometal halide perovskites." Science: 1228604.

Liu, M., M. B. Johnston and H. J. Snaith (2013). "Efficient planar heterojunction perovskite solar cells by vapour deposition." Nature 501(7467): 395.

Malinkiewicz, O., A. Yella, Y. H. Lee, G. M. Espallargas, M. Graetzel, M. K. Nazeeruddin and H. J. Bolink (2014). "Perovskite solar cells employing organic charge-transport layers." Nature Photonics 8(2): 128.

Noh, J. H., S. H. Im, J. H. Heo, T. N. Mandal and S. I. Seok (2013). "Chemical management for colorful, efficient, and stable inorganic–organic hybrid nanostructured solar cells." Nano letters 13(4): 1764-1769.

NREL Best Research-Cell Efficiencies, (accessed: April 2019).

https://www.nrel.gov/pv/assets/images/efficiency-chart.png.

Onozawa-Komatsuzaki, N., T. Funaki, T. N. Murakami, S. Kazaoui, M. Chikamatsu and K. Sayama (2017). "Novel Cobalt Complexes as a Dopant for Hole-transporting Material in Perovskite Solar Cells." Electrochemistry 85(5): 226-230.

Qi Jiang, Zema Chu, Pengyang Wang, Xiaolei Yang, Heng Liu, Ye Wang, Zhigang Yin, Jinliang Wu, Xinwang Zhang and Jingbi You (2017).” Planer-structure perovskite solar cells with efficiency beyond 21%”.

Qi Jiang, Xingwang Zhang, and Jingbi You (2018). “SnO2: A wonderful electron transport layer for perovskite cells”. Small, 1801154.

Roldan-Carmona, C., P. Gratia, I. Zimmermann, G. Grancini, P. Gao, M. Graetzel and M. K. Nazeeruddin (2015). "High efficiency methylammonium lead triiodide perovskite solar cells: the relevance of non-stoichiometric precursors." Energy & Environmental Science 8(12): 3550-3556.

Saliba, M.; Correa-Baena, J.-P.; Graetzel, M.; Hagfeldt, A.; Abate, A. Perovskite Solar Cells: From the Atomic Level to Film Quality and Device Performance. Angew. Chem., Int. Ed. 2018, 57, 2554−2569.

Saliba, M.; Matsui, T.; Domanski, K.; Seo, J.-Y.; Ummadisingu, A.; Zakeeruddin, S. M.; Correa-Baena, J.-P.; Tress, W. R.; Abate, A.; Hagfeldt, A.; Gratzel, M. Incorporation of rubidium cations into perovskite solar cells improves photovoltaic performance. Science 2016, 354, 206−209.

Shin, S. S.; Yeom, E. J.; Yang, W. S.; Hur, S.; Kim, M. G.; Im, J.; Seo, J.; Noh, J. H.; Seok, S. I. Colloidally prepared La-doped BaSnO3 electrodes for efficient, photostable perovskite solar cells. Science 2017, 356, 167−171.

Snaith, H. J. (2013). "Perovskites: the emergence of a new era for low-cost, high-efficiency solar cells." The Journal of Physical Chemistry Letters 4(21): 3623-3630.

Sum, T. C. and N. Mathews (2014). "Advancements in perovskite solar cells: photophysics behind the photovoltaics." Energy & Environmental Science 7(8): 2518-2534.

Tan, H.; Jain, A.; Voznyy, O.; Lan, X.; Garcia de Arquer, F. P.; Fan, J. Z.; Quintero-Bermudez, R.; Yuan, M.; Zhang, B.; Zhao, Y.; et al. Efficient and stable solution-processed planar perovskite solar cells via contact passivation. Science 2017, 355, 722−726.

Wenk, H.-R. and A. Bulakh (2016). Minerals: their constitution and origin, Cambridge University Press.

Xi, H., S. Tang, X. Ma, J. Chang, D. Chen, Z. Lin, P. Zhong, H. Wang and C. Zhang (2017). "Performance Enhancement of Planar Heterojunction Perovskite Solar Cells

through Tuning the Doping Properties of Hole-Transporting Materials." ACS Omega 2(1): 326336.

Yang, W. S., B.-W. Park, E. H. Jung, N. J. Jeon, Y. C. Kim, D. U. Lee, S. S. Shin, J. Seo, E. K. Kim and J. H. Noh (2017). "Iodide management in formamidinium-lead-halide–based perovskite layers for efficient solar cells." Science 356(6345): 1376-1379.

Zhou, H., Q. Chen, G. Li, S. Luo, T.-b. Song, H.-S. Duan, Z. Hong, J. You, Y. Liu and Y. Yang (2014). "Interface engineering of highly efficient perovskite solar cells." Science 345(6196): 542-546.

Zhu, Z., Y. Bai, X. Liu, C. C. Chueh, S. Yang and A. K. Y. Jen (2016). "Enhanced efficiency and stability of inverted perovskite solar cells using highly crystalline SnO_2 nanocrystals as the robust electron‐transporting layer." Advanced Materials 28(30): 64786484.

VITA

GUODUAN LIU

Education

M. Sc, Materials Physics, Sichuan University, Chengdu, China, Jun.2014.

Academic Appointments

Teaching Assistant, Department of Electrical and Computer Engineering, University of Kentucky, 01/2017-05/2019.

Publications

Guoduan Liu, Zili Kou, Xiaozhi Yan, Li Lei, Fang Peng, Qiming Wang, Kaixue Wang, Pei Wang, Yong Li, Liang Li, Wentao Li, Yonghua Wang, Yan Bi, Yang Leng and Duanwei He. “Submicron cubic boron nitride as hard as diamond”. Applied Physics Letters 106, 121901 (2015).